- Novel shell-cross-linked micelles with detachable PEG corona for glutathione-mediated intracellular drug delivery
  Wang, K.; Liu, Y.; Yi, W.-J.; Li, C.; Li, Y.-Y.; Zhuo, R.-X.; Zhang, X.-Z. *Soft Matter* **2013**, *9*, 692-699.
  Abstract:

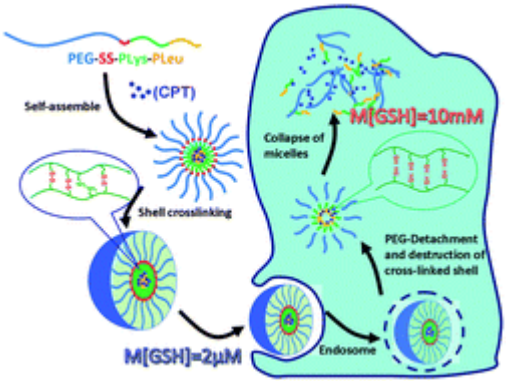

A series of novel disulfide-containing triblock copolymers, poly(ethylene glycol)-*b*-poly(L-lysine)-*b*-poly(*rac*-leucine) (PEG-SS-PLys-PLeu), were prepared. In an aqueous solution, the copolymers could self-assemble to form core–shell-corona micelles with a disulfide-linked detachable PEG corona, since the PLys middle shell with primary amine groups was linked by a disulfide-containing cross-linker. The morphology and stability of self-assembled micelles were characterized by TEM, DLS and SEM. In the intracellular environment, the micelles underwent destruction of the cross-linked shell with detachment of the PEG corona due to the cleavage of disulfide bonds, followed by the collapse of micelles. The *in vitro* drug release in response to GSH was further studied. Interestingly, it was found that the micelles not only exhibited reduced drug loss in extracellular environments, but also drastically accelerated drug release at the cytoplasmic GSH level, leading to enhanced growth inhibition of HeLa cells. The glutathione-responsive micelles might have great potential in intracellular drug delivery.

- Amphiphilic star-shaped block copolymers as unimolecular drug delivery systems: investigations using a novel fungicide
  Knop, K.; Pavlov, G. M.; Rudolph, T.; Martin, K.; Pretzel, D.; Jahn, B. O.; Scharf, D. H.; Brakhage, A. A.; Makarov, V.; Möllmann, U.; Schacher, F. H.; Schubert, U. S. *Soft Matter* **2013**, *9*, 715-726.
  Abstract:

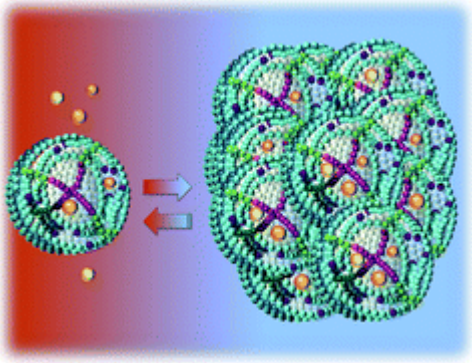

Amphiphilic star-shaped poly(ε-caprolactone)-*block*-poly(oligo(ethylene glycol)methacrylate) [PCL_a-*b*-$POEGMA_b$]$_4$ block copolymers with four arms and varying degrees of polymerization for the core

(PCL) and the shell (POEGMA) were used to investigate the solution behavior in dilute aqueous solution using a variety of techniques, including fluorescence and UV/Vis spectroscopy, dynamic light scattering, analytical ultracentrifugation, and isothermal titration calorimetry. Particular emphasis has been applied to prove that the systems form unimolecular micelles for different hydrophilic/lipophilic balances of the employed materials. *In vitro* cytotoxicity and hemocompatibility have further been investigated to probe the suitability of these structures for *in vivo* applications. A novel fungicide was included into the hydrophobic core in aqueous media to test their potential as drug delivery systems. After loading, the materials have been shown to release the drug and to provoke therewith an inhibition of the growth of different fungal strains.

- A Simple Route to Synthesize Mesoporous ZSM-5 Templated by Ammonium-Modified Chitosan
  Jin, J.; Zhang, X.; Li, Y., Li, H.; Wu, W.; Cui, Y.; Chen, Q.; Li, L.; Gu, J.; Zhao, W.; Shi, J. *Chem. Eur. J.* **2012**, *18*, 16549–16555.
  Abstract:

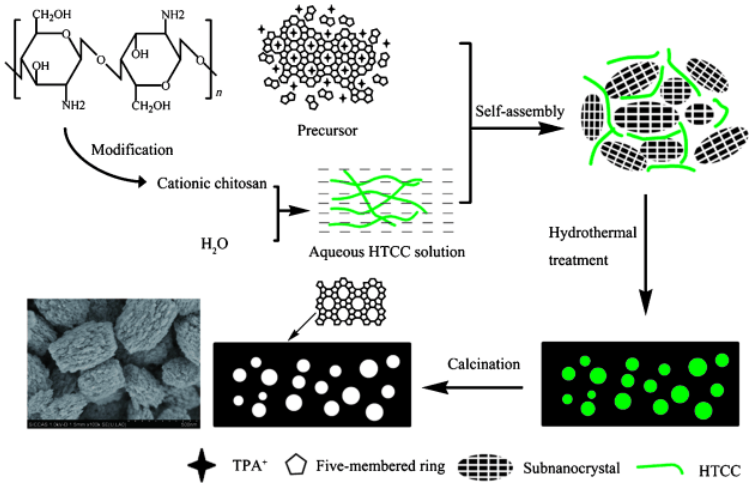

Uniform mesoporous zeolite ZSM-5 crystals have been successfully fabricated through a simple hydrothermal synthetic method by utilizing ammonium-modified chitosan and tetrapropylammonium hydroxide (TPAOH) as the meso- and microscale template, respectively. It was revealed that mesopores with diameters of 5–20 nm coexisted with microporous network within mesoporous ZSM-5 crystals. Ammonium-modified chitosan was demonstrated to serve as a mesoporogen, self-assembling with the zeolite precursor through strong static interactions. As expected, the prepared mesoporous ZSM-5 exhibited greatly enhanced catalytic activities compared with conventional ZSM-5 and Al-MCM-41 in reactions involving bulky molecules, such as the Claisen–Schmidt condensation of 2-hydroxyacetophenone with benzaldehyde and the esterification reaction of dodecanoic acid and 2-ethylhexanol.

- Phosphorylated 3-Heteroarylcoumarins and Their Use in Fluorescence Microscopy and Nanoscopy
  Nizamov, S.; Willig, K. I.; Sednev, M. V.; Belov, V. N.; Hell, S. W. *Chem. Eur. J.* **2012**, *18*, 16339–16348.
  Abstract:

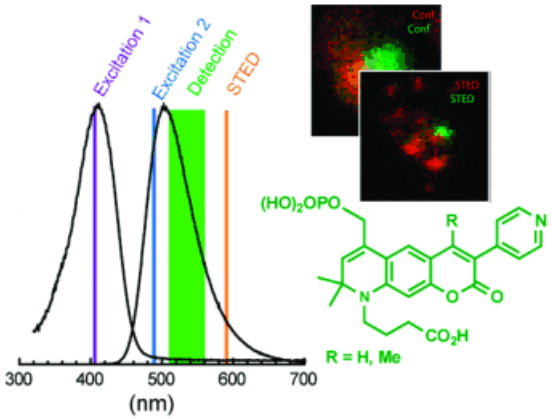

Photostable and bright fluorescent dyes with large Stokes shifts are widely used as markers in far-field optical microscopy, but the variety of useful dyes is limited. The present study introduces new 3-heteroaryl coumarins decorated with a primary phosphate group ($OP(O)(OH)_2$) attached to C-4 in 2,2,4-trimethyl-1,2-dihydroquinoline fragment fused with the coumarin fluorophore. The general synthetic route is based on the Suzuki reaction of 3-bromocoumarines with hetarylboronic acids followed by oxidation of the methyl group at the C═C bond with SeO_2 (to an aldehyde), reduction with $NaBH_4$ (to an alcohol), and conversion into a primary phosphate. The 4 position in the coumarin system may be unsubstituted or bear a methyl group. Phosphorylated coumarins were found to have high fluorescence quantum yields in the free state and after conjugation with proteins (in aqueous buffers). In super-resolution light microscopy with stimulated emission depletion (STED), the new coumarin dyes provide an optical resolution of 40–60 nm with a low background signal. Due to their large Stokes shifts and high photostability, phosphorylated coumarins enable to combine multilabel imaging (using one detector and several excitation sources) with diffraction unlimited optical resolution.

- Reversible Phase Transformation and Luminescence of Cadmium(II)–Dipyridylamide-Based Coordination Frameworks
  Tzeng, B.-C.; Wie, S.-L.; Chang, T.-Y. *Chem. Eur. J.* **2012**, *18*, 16443–16449.
  Abstract:

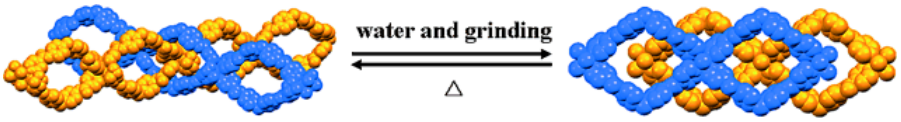

We have synthesized a series of 1D double-zigzag $(\{[Cd(paps)_2(H_2O)_2](ClO_4)_2\}_n$ (**1**), $\{[Cd(papo)_2(H_2O)_2](ClO_4)_2\}_n$ (**3**), and $\{[Cd(papc)_2(H_2O)_2](ClO_4)_2\}_n$ (**5**)) and 2D polyrotaxane frameworks ($[Cd(papc)_2(ClO_4)_2]_n$ (**6**)) by the reaction of $Cd(ClO_4)_2$ with dipyridylamide ligands *N*,*N*′-bis(pyridylcarbonyl)-4,4′-diaminodiphenyl thioether (paps), *N*,*N*′-bis(pyridylcarbonyl)-4,4′-diaminodiphenyl ether (papo), and *N*,*N*′-(methylenedi-*p*-phenylene)bispyridine-4-carboxamide (papc), respectively, where their molecular structures have been determined by X-ray diffraction studies. Based on the powder X-ray data (PXRD) of compound **3** and its Zn^{II} analogue, heating the double-zigzag framework of compound **3** can give the polyrotaxane framework of $[Cd(papo)_2(ClO_4)_2]_n$ (**4**) and grinding this powder sample in the presence of moisture resulted in its complete conversion back into the pure double-zigzag framework. In addition, heating the double-zigzag frameworks of compounds **1** and **5** can induce structural transformation into their respective polyrotaxanes, whereas grinding these solid samples in the presence of moisture did not lead to the formation of the double zigzags. Herein, we investigated the effect of the metal (from Zn^{II} to Cd^{II}) on the assembly

process and luminescence properties, as well as on the particularly intriguing structural transformation of a series of papx-based frameworks. In fact, the assembly behavior and luminescence properties of the Cd^{II}—papx and Zn^{II}—papx frameworks were really similar. However, both Zn^{II}—papx (x=s, o) frameworks can perform reversible structural transformation, but only the Cd^{II}—papo framework can do it. Therefore, a delicate metal effect on such a new structural transformation can be observed.

- Photoreductive Uncaging of Fluorophore in Response to Protein Oligomers by Templated Reaction in Vitro and in Cellulo
  Sadhu, K. K.; Eierhoff, T.; Römer, W.; Winssinger, N. *J. Am. Chem. Soc.* **2012**, *134*, 20013–20016.
  Abstract:

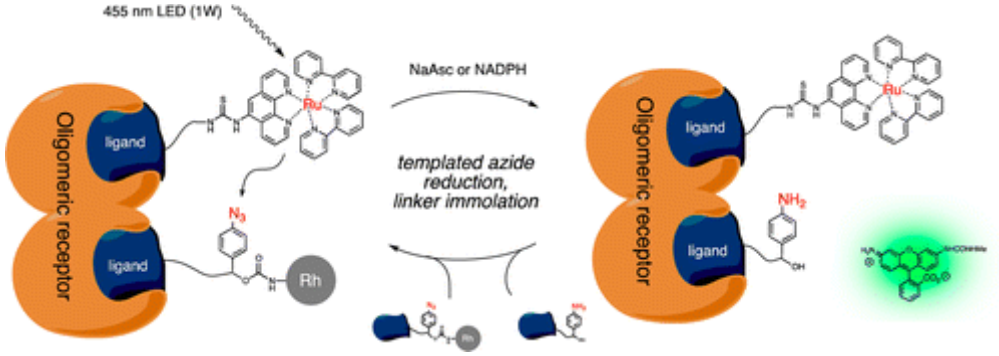

The photoreduction of azide-based immolative linker by Ru(II) conjugates to uncage rhodamine was achieved using different oligomeric protein templates. The generality of the approach was validated with three sets of ligand having varying affinity to their target (biotin, desthiobiotin and raloxifene). The reaction rates of the templated reaction was found to be at least 30-fold faster than the untemplated reaction providing a clear fluorescent signal in response to the protein oligomer within 30 min. The templated reaction was found to also proceed in cellulo and could be used to identify acetyl coenzyme A carboxylase (ACC) in Pseudomonas aeruginosa and human cell lines as well the and estrogen receptor (ER).

- Supramolecular Sensor for Cancer-Associated Nitrosamines
  Minami, T.; Esipenko, N. A.; Zhang, B.; Kozelkova, M. E.; Isaacs, L.; Nishiyabu, R.; Kubo, Y.; Anzenbacher, P. *J. Am. Chem. Soc.* **2012**, *134*, 20021–20024.
  Abstract:

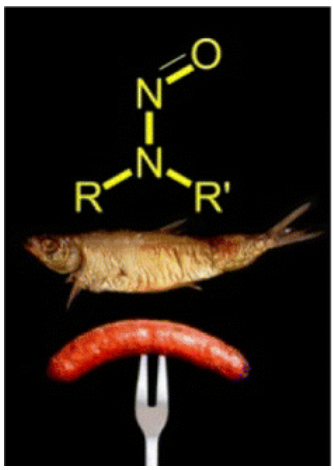

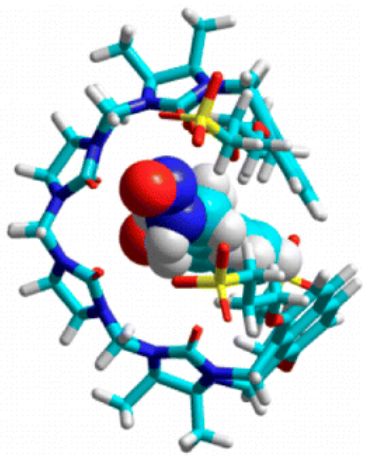

A supramolecular assay based on two fluorescent cucurbit[n]uril probes enables the recognition and quantification of nitrosamines, including cancer-associated nitrosamines, compounds that are difficult to recognize. The cross-reactive sensor leverages weak interactions and competition among the probe, metal, and guest, yielding high information density in the signal output (variance) and enabling the recognition of structurally similar guests.

- Thermo-Induced Self-Assembly of Responsive Poly(DMAEMA-*b*-DEGMA) Block Copolymers into Multi- and Unilamellar Vesicles
  Pietsch, C.; Mansfeld, U.; Guerrero-Sanchez, C.; Hoeppener, S.; Vollrath, A.; Wagner, M.; Hoogenboom, R.; Saubern, S.; Thang, S.-H.; Chiefari, J.; Schubert, U. S. *Macromolecules* **2012**, *45*, 9292–9302.
  Abstract:

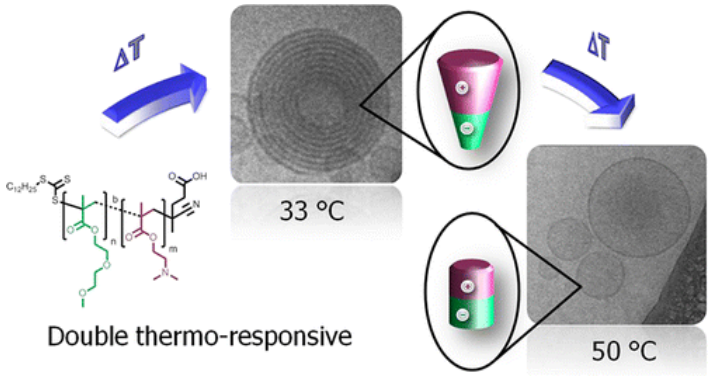

A series of thermoresponsive diblock copolymers of poly[2-(dimethylamino)ethyl methacrylate-*block*-di(ethyleneglycol) methyl ether methacrylate], poly(DMAEMA-*b*-DEGMA), were synthesized by reversible addition–fragmentation chain transfer (RAFT) polymerizations. The series consist of diblock and quasi diblock copolymers. Sequential monomer addition was used for the quasi diblock copolymer synthesis and the macro-chain transfer approach was utilized for the block copolymer synthesis. The focus of this contribution is the controlled variation of the ratios of DMAEMA to DEGMA in the copolymer composition, resulting in a systematic polymer library. One of the investigated block copolymer systems showed double lower critical solution temperature (LCST) behavior in water and was further investigated. The phase transitions of this block copolymer were studied in aqueous solutions by turbidimetry, dynamic light scattering (DLS), variable temperature proton nuclear magnetic resonance (^{1}H NMR) spectroscopy, zeta potential, and cryo transmission electron microscopy (cryo-TEM). The block copolymer undergoes a two-step thermo-induced self-assembly, which results in the formation of multilamellar vesicles after the first LCST temperature and to unilamellar vesicles above the second LCST transition. An interplay of ionic interactions as well as the change of the corresponding volume fraction during the LCST transitions were identified as the driving force for the double responsive behavior.

- Organic/Inorganic Hybrid Block Copolymer Electrolytes with Nanoscale Ion-Conducting Channels for Lithium Ion Batteries
  Kim, S.-K.; Kim, D.-G.; Lee, A.; Sohn, H.-S.; Wie, J.-J.; Nguyen, N. A.; Mackay, M. E.; Lee, J.-C. *Macromolecules* **2012**, *45*, 9347–9356.
  Abstract:

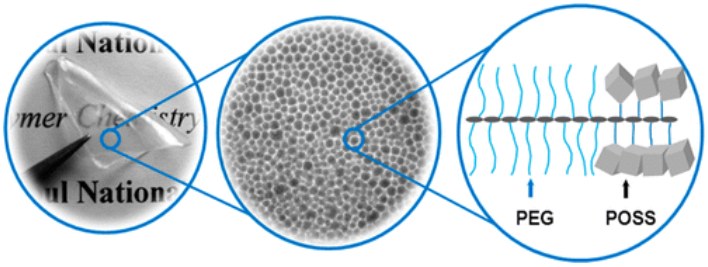

A series of organic/inorganic hybrid block and random copolymers were prepared by reversible addition–fragmentation chain transfer (RAFT) polymerization using poly(ethylene glycol) methyl ether methacrylate (PEGMA) and 3-(3,5,7,9,11,13,15-heptaisobutylpentacyclo[9.5.1.1^{3,9}.1^{5,15}.1^{7,13}]octasiloxane-1-yl)propyl methacrylate (MA-POSS) as monomers in order to study the effect of polymer morphology and POSS content on the properties of polymer electrolytes. Flexible and dimensionally stable free-standing films were made from the hybrid block and random copolymers mixed with lithium bis(trifluoromethanesulfonyl)imide (LiTFSI) when the contents of MA-POSS unit were larger than 31 and 16 mol %, respectively. The ionic conductivity of the solid-state block copolymer (PBP) electrolyte was found to be 1 order of magnitude higher than that of the random copolymer (PRP) electrolyte when they had similar MA-POSS content, although their glass transition temperature values of their ion-conducting segments were quite close. Moreover, the ionic conductivity of the PBP electrolyte was not much different from that of the wax state poly(poly(ethylene glycol) methyl ether methacrylate) (P(PEGMA)) electrolyte. For example, the ionic conductivity values for the PBP electrolyte containing 31 mol % of MA-POSS, the PRP electrolyte containing 29 mol % of MA-POSS, and P(PEGMA) electrolyte were 2.05 × 10^{-5}, 3.00 × 10^{-6}, and 4.23 × 10^{-5} S cm^{-1}, respectively, at 30 °C. The large ionic conductivity value of the block copolymer electrolyte is ascribed to the nanophase separation forming the ion-conducting channels.

- Significance of the Amide Functionality on DOPA-Based Monolayers on Gold
  Rıbena, D.; Alekseev, A.; Van Asselen, O.; Mannie, G. J. A.; Hendrix, M. M. R. M.; Van der Ven, L. G. J.; Sommerdijk, N. A. J. M.; De With, G. *Langmuir* **2012**, *28*, 16900–16908.
  Abstract:

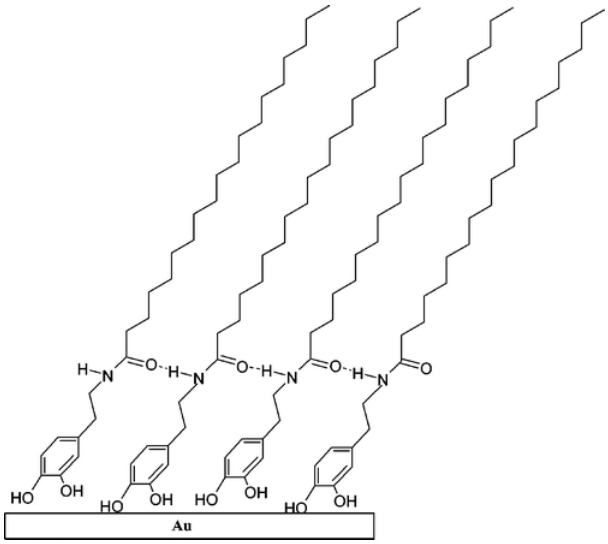

The adhesive proteins secreted by marine mussels contain an unusual amino acid, 3,4-dihydroxyphenylalanine (DOPA), that is responsible for the cohesive and adhesive strength of this

natural glue and gives mussels the ability to attach themselves to rocks, metals, and plastics. Here we report a detailed structural and spectroscopic investigation of the interface between *N*-stearoyldopamine and a single-crystalline Au(111) model surface and an amide-absent molecule, 4-stearylcatechol, also on Au(111), with the aim of understanding the role of the amide functionality in the packing, orientation, and fundamental interaction between the substrate and the monolayer formed from an aqueous environment by the Langmuir–Blodgett technique. The organization of monolayers on gold was observed directly and studied in detail by X-ray photoelectron spectroscopy (XPS), contact angle measurements (CA), surface-enhanced Raman spectroscopy (SERS), infrared reflection–absorption spectroscopy (IRRAS), and atomic force microscopy (AFM). Our study shows that within the monolayer the catecholic oxygen atoms are coordinated to the gold surface, having a more perpendicular orientation with respect to the aromatic ring and the apparently tilted alkyl chains, whereas the amide functionality stabilizes the monolayer that is formed.

- Platinum Electrodeposition on Unsupported Carbon Nano-Onions
  Santiago, D.; Rodríguez-Calero, G. G.; Palkar, A.; Barraza-Jimenez, D.; Galvan, D. H.; Casillas, G.; Mayoral, A.; Jose-Yacamán, M.; Echegoyen, L.; Cabrera, C. R. *Langmuir* **2012**, *28*, 17202–17210.
  Abstract:

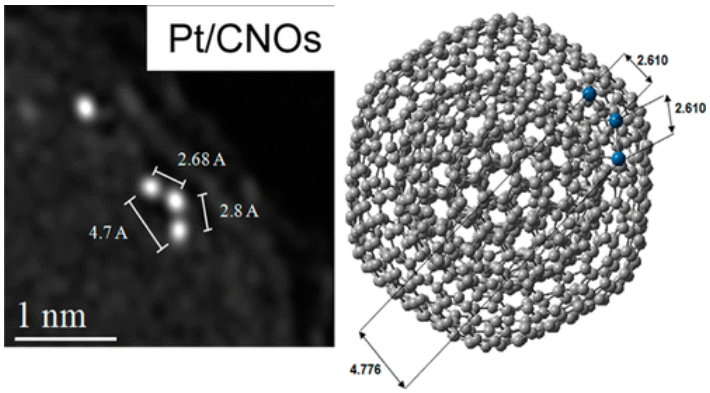

An effort to develop smaller, well-dispersed catalytic materials electrochemically on high-surface-area carbon supports is required for improved fuel cell performance. A high-surface-area carbon material of interest is carbon nano-onions (CNOs), also known as multilayer fullerenes. The most convenient synthesis method for CNOs is annealing nanodiamond particles, thus retaining the size of the precursors and providing the possibility to prepare very small nanocatalysts using electrochemical techniques. In terms of pure metal catalysts, platinum is the most common catalyst used in fuel cells. The combination of Pt nanoparticles with CNOs could lead to new catalytic nanomaterials. In this work, this was accomplished by using a rotating disk–slurry electrode (RoDSE) technique. The Pt/CNO catalysts were prepared from slurries that contained functionalized CNOs and K_2PtCl_6 as the platinum precursor in aqueous 0.1 M H_2SO_4 solution. X-ray photoelectron spectroscopy results showed that 37% of the Pt on the CNOs is metallic Pt whereas 63% had higher binding energies, which is evidence of higher oxidation states or the presence of Pt atoms and clusters on CNOs. However, aberration-corrected scanning transmission electron microscopy of the Pt/CNOs confirmed the presence of Pt atoms and clusters on CNOs. Thermal gravimetric analysis showed the excellent thermal stability of the Pt/CNOs and a lower onset potential for the electrochemical oxidation of methanol compared to that of commercial Pt/Vulcan catalyst material. The computational method confirmed the Pt atoms' location at CNOs surface sites. Geometric

parameters for distances between Pt atoms in the 3Pt/CNOs molecular system from our theoretical calculations are in agreement with the respective parameters obtained experimentally. The combination of CNO with RoDSE presents a new highly dispersed catalyst nanomaterial.

- pH-Programmable DNA Logic Arrays Powered by Modular DNAzyme Libraries
  Elbaz, J.; Wang, F.; Remacle, F.; Willner, I. *Nano Letters* **2012**, *12*, 6049-6054.
  Abstract:

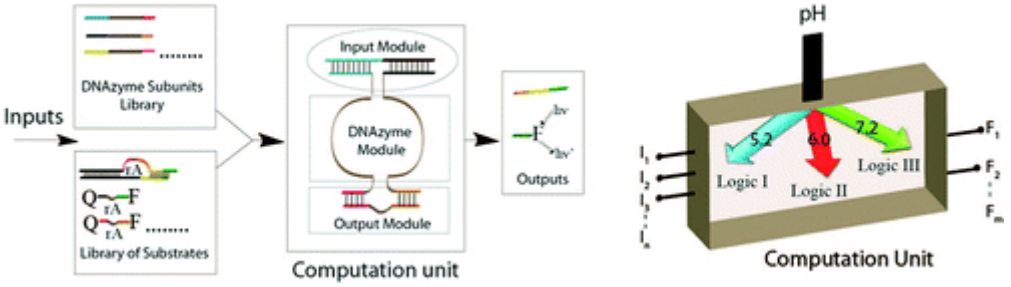

Nature performs complex information processing circuits, such the programmed transformations of versatile stem cells into targeted functional cells. Man-made molecular circuits are, however, unable to mimic such sophisticated biomachineries. To reach these goals, it is essential to construct programmable modular components that can be triggered by environmental stimuli to perform different logic circuits. We report on the unprecedented design of artificial pH-programmable DNA logic arrays, constructed by modular libraries of Mg^{2+}- and UO_2^{2+}-dependent DNAzyme subunits and their substrates. By the appropriate modular design of the DNA computation units, pH-programmable logic arrays of various complexities are realized, and the arrays can be erased, reused, and/or reprogrammed. Such systems may be implemented in the near future for nanomedical applications by pH-controlled regulation of cellular functions or may be used to control biotransformations stimulated by bacteria.

- Direct Imaging of DNA Fibers: The Visage of Double Helix
  Gentile, F.; Moretti, M.; Limongi, T.; Falqui, A.; Bertoni, G.; Scarpellini, A.; Santoriello, S.; Maragliano, L.; Proietti Zaccaria, R.; di Fabrizio, E. *Nano Letters* **2012**, *12*, 6453-6458.
  Abstract:

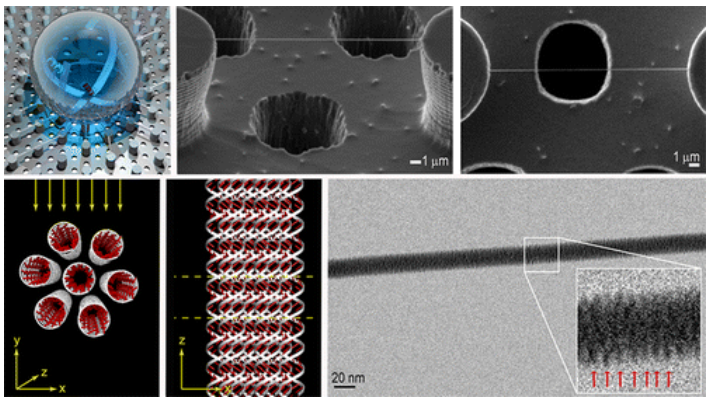

Direct imaging becomes important when the knowledge at few/single molecule level is requested and where the diffraction does not allow to get structural and functional information. Here we report on the direct imaging of double stranded (ds) λ-DNA in the A conformation, obtained by combining a novel sample preparation method based on super hydrophobic DNA molecules self-aggregation process with transmission electron microscopy (TEM). The experimental breakthrough is the

production of robust and highly ordered paired DNA nanofibers that allowed its direct TEM imaging and the double helix structure revealing.

- Three-Dimensional Nanographene Based on Triptycene: Synthesis and Its Application in Fluorescence Imaging
  Zhang, C.; Liu, Y.; Xiong, X.-Q.; Peng, L.-H.; Gan, L.; Chen, C.-F.; Xu, H.-B. *Org. Lett.* **2012**, *14*, 5912–5915.
  Abstract:

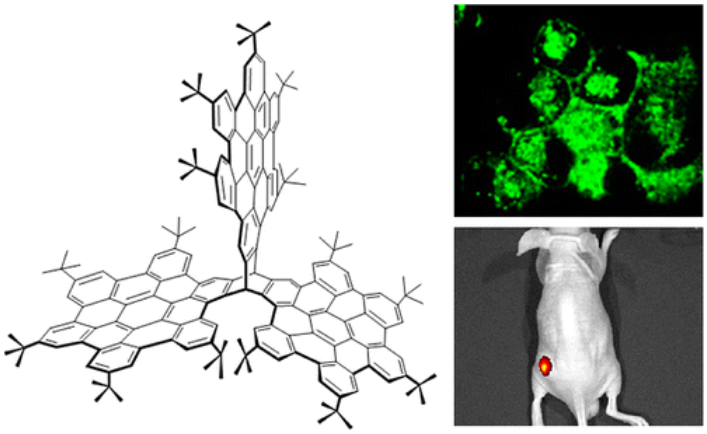

A novel kind of three-dimensional (3D) nanographene based on a triptycene structure bearing three hexa-peri-hexabenzocoronene (HBC) moieties was synthesized efficiently from triiodotriptycene. With the characteristic of intrinsic fluorescence, the 3D nanographene was used as a fluorescent agent for in vitro and in vivo fluorescence imaging with good antiphotobleaching ability and little toxicity.

- Total Synthesis of the Proposed Structure of Roxbin B; the Nonidentical Outcome
  Yamaguchi , S.; Ashikaga, Y.; Nishii, K.; Yamada, H. *Org. Lett.* **2012**, *14*, 5928–5931.
  Abstract:

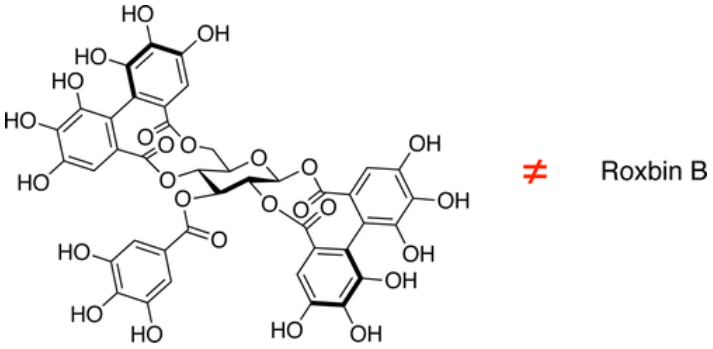

A proposed structure of roxbin B was synthesized. For the synthesis, a new synthetic method for the preparation of the hexahydroxydiphenoyl (HHDP) bridge was developed that involved the stepwise esterification of axially chiral HHDP acid anhydride. The synthesized compound was not identical to the natural roxbin B.

- Enhancement and Modulation of Enzymatic Activity through Higher-Order Structural Changes of Giant DNA–Protein Multibranch Conjugates
  Rudiuk, S.; Venancio-Marques, A.; Baigl, D. *Angew. Chem. Int. Ed.* **2012**, *51*, 12694–12698.
  Abstract:

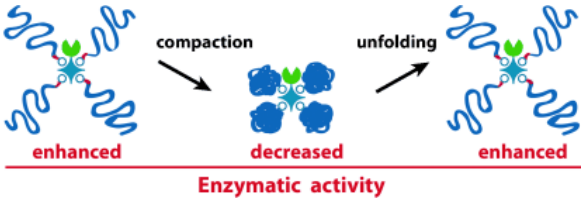

A giant DNA leap for enzyme-kind: Giant DNA–protein multibranch conjugates were shown to be composed of a single β-lactamase enzyme (green, see scheme) conjugated to up to four 48.5 kbp lambda phage DNA branches (blue lines). The conjugation of giant DNA induces a two- to fourfold enhancement of the enzymatic activity, which is modulated by changes in the higher-order DNA structure.

- Highly Efficient Ultrafast Electron Injection from the Singlet MLCT Excited State of Copper(I) Diimine Complexes to TiO_2 Nanoparticles
  Huang, J.; Buyukcakir, O.; Mara, M. W.; Coskun, A.; Dimitrijevic, N. M.; Barin, G.; Kokhan, O.; Stickrath, A. B.; Ruppert, R.; Tiede, D. M.; Stoddart, J. F.; Sauvage, J.-P.; Chen, L. X. *Angew. Chem. Int. Ed.* **2012**, *51*, 12711–12715.
  Abstract:

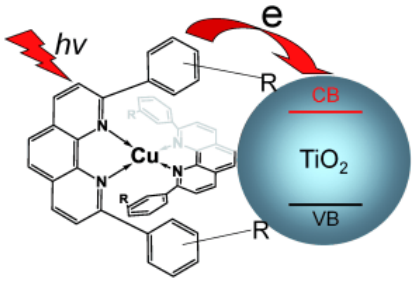

Cu complexes as photosensitizers: Photoinduced charge-transfer dynamics from a copper(I) diimine complex to TiO_2 nanoparticles were investigated by combining multiple time-resolved spectroscopic methods. An efficient and ultrafast electron transfer process from the singlet MLCT state was discovered as a result of structural control owing to the flattening of the tetrahedral geometry in the complex and the bulky groups in the ligands.

- Photocatalytic Conversion of Diluted CO_2 into Light Hydrocarbons Using Periodically Modulated Multiwalled Nanotube Arrays
  Zhang, X.; Han, F.; Shi, B.; Farsinezhad, S.; Dechaine, G. P.; Shankar, K. *Angew. Chem. Int. Ed.* **2012**, *51*, 12732–12735.
  Abstract:

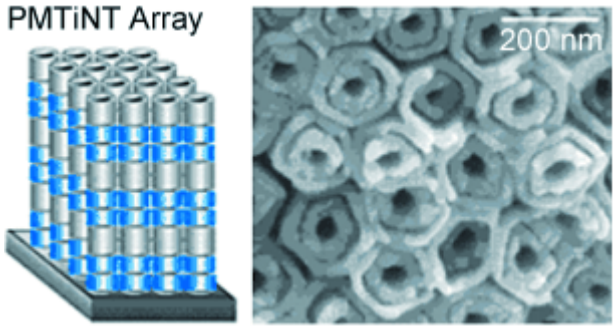

Cu–Pt bimetallic shells supported on a double-walled TiO_2 nanotube (PMTiNT) array are efficient photocatalysts for the room-temperature conversion of CO_2 into light hydrocarbons, such as CH_4,

C_2H_4, and C_2H_6. When $Cu_{0.33}$–$Pt_{0.67}$/PMTiNT was used for the photoreduction of diluted CO_2 (1□% in N_2), an average hydrocarbon production rate of 3.7 mL□g^{-1}□h^{-1} or 6.1 mmol□m^{-2}□h^{-1} was realized under AM□1.5 one-sun illumination.

- Coupling Dy_3 Triangles to Maximize the Toroidal Moment
  Lin, S.-Y.; Wernsdorfer, W.; Ungur, L.; Powell, A. K.; Guo, Y.-N.; Tang, J.; Zhao, L.; Chibotaru, L. F.; Zhang, H.-J. *Angew. Chem. Int. Ed.* **2012**, *51*, 12767–12771.
  Abstract:

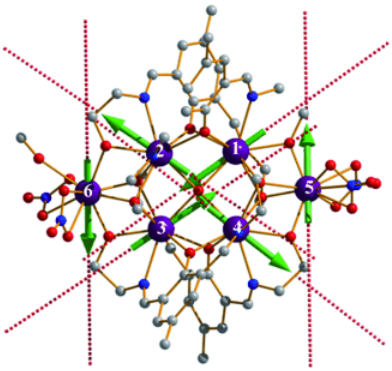

A hexanuclear dysprosium(III) compound constructed by two Dy_3 triangles in an edge-to-edge arrangement perfectly retains a nonmagnetic ground state and single-molecular-magnet behavior. Such an arrangement and the strong couplings over a μ_4-O^{2-} ion stabilize a similar arrangement of toroidal moments in the ground state, thus maximizing the toroidal moment of the complex. (Picture: Dy purple, C gray, N blue, O red.)

- Effect of Axial Interactions on the Formation of Mesophases: Comparison of the Phase Behavior of Dialkyl 2,2□-bipyridyl-4,4□-dicarboxylate Complexes of Pt(II), Pt(IV), and Pt(II)/Pt(IV) Molecular Alloys
  Allenbaugh, R. J.; Schauer, C. K.; Josey, A.; Martin, J. D.; Anokhin, D. V.; Ivanov, D. A. *Chem. Mater.* **2012**, *24*, 4517–4530.
  Abstract:

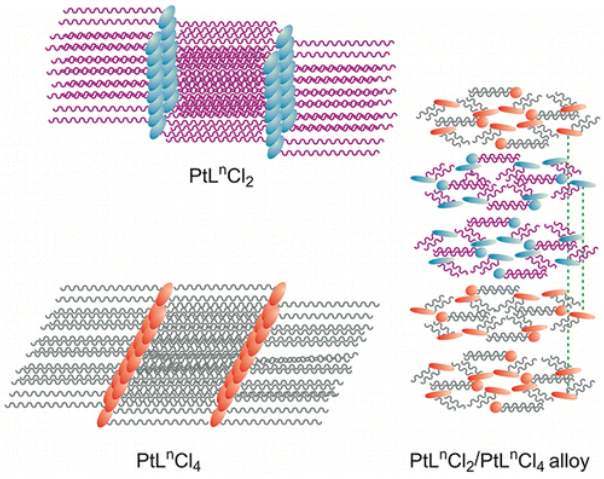

Crystal engineering through the use of metal-based interactions is relatively common, but this approach has not been widely used to develop highly ordered liquid-crystalline (LC) phases. Herein is presented a Pt(II)/Pt(IV) system with a highly ordered LC phase engineered to form through metal-based MX chain interactions of the type Pt(II)···Cl-Pt(IV). This LC material constitutes a molecular

alloy in which a single mesophase is formed from two components, and is the first alloy to include a Pt(IV) component. The molecular alloy was characterized via differential scanning calorimetry (DSC), polarizing optical microscopy (POM), and variable-temperature X-ray diffraction (VT XRD). The alloy properties are contrasted with complimentary analyses of the individual components. The newly synthesized tetrachloro(dialkyl 4,4′-dicarboxylate-2,2′-bipyridyl)platinum(IV) complexes (PtL*n*Cl_4, n is the number of carbons in the alkyl chain) are themselves liquid crystalline. Structural and thermal properties of the Pt(II) analogues are presented to provide context to the behaviors of the Pt(IV) species and the alloys. Single-crystal X-ray diffraction data is presented for $PtL^1Cl_2{\cdot}CH_2Cl_2$, PtL^2Cl_2, and $PtL^{16}Cl_2{\cdot}\bullet 2CHCl_3$. This study demonstrates the potential of mesophase ordering through carefully engineered metal-based interactions. The resulting alloy provides a phase for studying MX chain interactions outside of the solid state.

- Fabrication of Binary and Ternary Hybrid Particles Based on Colloidal Lithography
  Yu, Y.; Ai, B.; Möhwald, H.; Zhou, Z.; Zhang, G.; Yang B. *Chem. Mater.* **2012**, *24*, 4549–4555.
  Abstract:

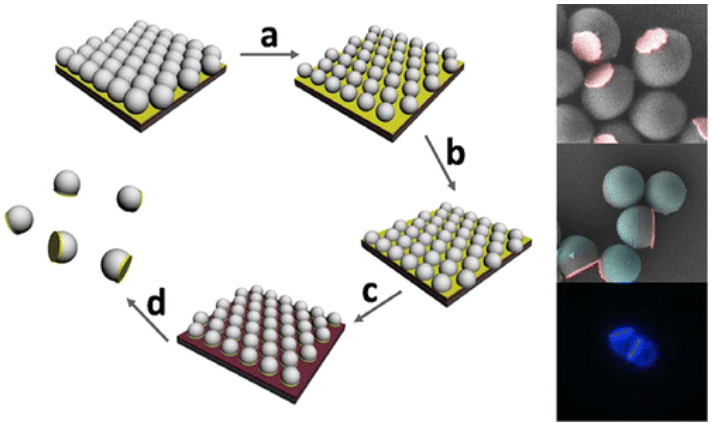

We describe a versatile strategy for engineering binary and ternary hybrid particles (HPs) through a combination of etching and deposition processes based on colloidal lithography (CL). Non-close-packed (ncp) polymer colloidal crystals were used as both original seed microparticles and templates for generating hybrid patches. Utilizing chemical or plasmonic etching procedures, the hybrid patches were generated underneath the colloidal template and were successfully attached on the microspheres through thermal treatment. The hybrid particles composing metals and polymers were tunable in size, composition, and morphology. This method provides a versatile and modular tool to fabricate similar hybrid microparticles and/or nanoparticles that, integrated into predesigned materials, promise applications in photonic and magnetic devices.

- Microfluidic Fabrication of Self-Assembled Peptide-Polysaccharide Microcapsules as 3D Environments for Cell Culture
  Mendes, A. C.; Baran, E. T.; Lisboa, P.; Reis, R. L.; Azevedo, H. S. *Biomacromolecules* **2012**, *13*, 4039–4048.
  Abstract:

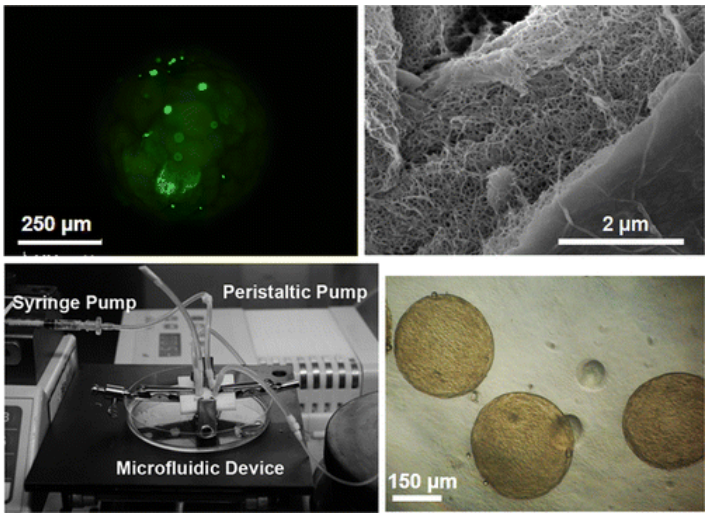

We report a mild cell encapsulation method based on self-assembly and microfluidics technology. Xanthan gum, an anionic polysaccharide, was used to trigger the self-assembly of a positively charged multidomain peptide. The self-assembly resulted in the formation of a nanofibrous matrix and using a microfluidic device, microcapsules with homogeneous size were fabricated. The properties and performance of xanthan-peptide microcapsules were optimized by changing peptide/polysaccharide ratio and their effects on the microcapsule permeability and mechanical stability were analyzed. The effect of microcapsule formulation on viability and proliferation of encapsulated chondrocytic (ATDC5) cells was also investigated. The encapsulated cells were metabolically active, showing an increased viability and proliferation over 21 days of in vitro culture, demonstrating the long-term stability of the self-assembled microcapsules and their ability to support and enhance the survival of encapsulated cells over a prolonged time. Self-assembling materials combined with microfluidics demonstrated to be an innovative approach in the fabrication of cytocompatible matrix for cell microencapsulation and delivery.

- Supramolecular Organization in Self-Assembly of Chromatin and Cationic Lipid Bilayers is Controlled by Membrane Charge Density
  Berezhnoy, N. V.; Lundberg, D.; Korolev, N.; Lu, C.; Yan, J.; Miguel, M.; Lindman, B.; Nordenskiöld, L. *Biomacromolecules* **2012**, *13*, 4146–4157.
  Abstract:

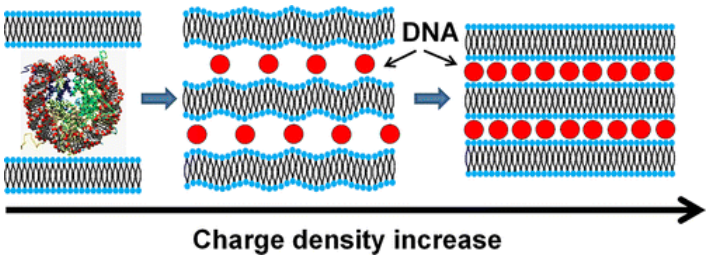

In this work we have investigated the structures of aggregates formed in model systems of dilute aqueous mixtures of “model chromatin” consisting of either recombinant nucleosome core particles (NCPs) or nucleosome arrays consisting of 12 NCPs connected with 30 bp linker DNA, and liposomes made from different mixtures of cationic and zwitterionic lipids, 1,2-dioleoyl-3-trimethylammonium-propane chloride salt (DOTAP) and 1,2-dioleoyl-sn-glycero-3-phosphocholine (DOPC). The aggregates formed were characterized using different optical microscopy methods and small-angle X-ray scattering (SAXS), and the results are discussed in terms of the competing intermolecular interactions

among the components. For a majority of the samples, the presence of lamellar structures could be identified. In samples with high fractions of DOTAP in the liposomes, well-defined lamellar structures very similar to those formed by the corresponding lipid mixtures and DNA alone (i.e., without histone proteins) were observed; in these aggregates, the histones are expelled from the model chromatin. The findings suggest that, with liposomes containing large fractions of cationic lipid, the dominating driving force for aggregation is the increase in translational entropy from the release of counterions, whereas with lower fractions of the cationic lipid, the entropy of mixing of the lipids within the bilayers results in a decreased DNA–lipid attraction.

- Structurally ordered intermetallic platinum–cobalt core–shell nanoparticles with enhanced activity and stability as oxygen reduction electrocatalysts
  Wang, D.; Xin, H. L.; Hovden, R.; Wang, H.; Yu, Y.; Muller, D. A.; DiSalvo, F. J.; Abruña, H. D. *Nature Materials* **2013**, *12*, 81–87.
  Abstract:

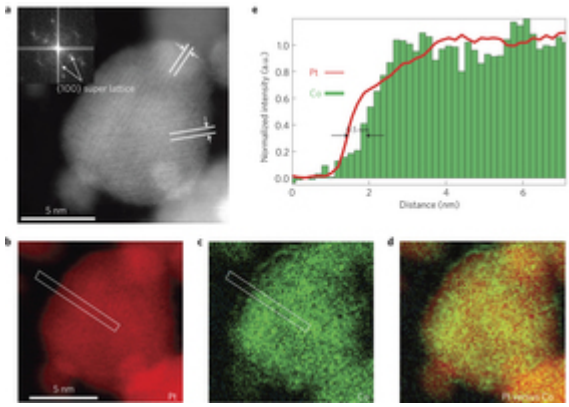

To enhance and optimize nanocatalyst performance and durability for the oxygen reduction reaction in fuel-cell applications, we look beyond Pt–metal disordered alloys and describe a new class of Pt–Co nanocatalysts composed of ordered Pt_3Co intermetallic cores with a 2–3 atomic-layer-thick platinum shell. These nanocatalysts exhibited over 200% increase in mass activity and over 300% increase in specific activity when compared with the disordered Pt_3Co alloy nanoparticles as well as Pt/C. So far, this mass activity for the oxygen reduction reaction is the highest among the Pt–Co systems reported in the literature under similar testing conditions. Stability tests showed a minimal loss of activity after 5,000 potential cycles and the ordered core–shell structure was maintained virtually intact, as established by atomic-scale elemental mapping. The high activity and stability are attributed to the Pt-rich shell and the stable intermetallic Pt_3Co core arrangement. These ordered nanoparticles provide a new direction for catalyst performance optimization for next-generation fuel cells.

- P2-Na_xVO_2 system as electrodes for batteries and electron-correlated materials
  Guignard, M.; Didier, C.; Darriet, J.; Bordet, P.; Elkaïm, E.; Delmas C. *Nature Materials* **2013**, *12*, 74–80.
  Abstract:

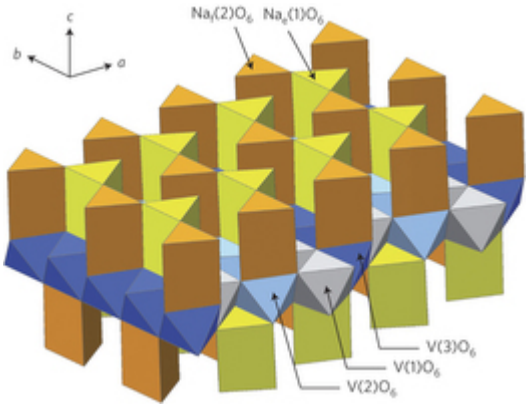

Layered oxides are the subject of intense studies either for their properties as electrode materials for high-energy batteries or for their original physical properties due to the strong electronic correlations resulting from their unique structure. Here we present the detailed phase diagram of the layered P2-Na_xVO_2 system determined from electrochemical intercalation/deintercalation in sodium batteries and *in situ* X-ray diffraction experiments. It shows that four main single-phase domains exist within the $0.5 \leq x \leq 0.9$ range. During the sodium deintercalation (intercalation), they differ from one another in the sodium/vacancy ordering between the VO_2 slabs, which leads to commensurable or incommensurable superstructures. The electrochemical curve reveals that three peculiar compositions exhibit special structures for x = 1/2, 5/8 and 2/3. The detailed structural characterization of the P2-$Na_{1/2}VO_2$ phase shows that the Na^+ ions are perfectly ordered to minimize Na^+/Na^+ electrostatic repulsions. Within the VO_2 layers, the vanadium ions form pseudo-trimers with very short V–V distances (two at 2.581 Å and one at 2.687 Å). This original distribution leads to a peculiar magnetic behaviour with a low magnetic susceptibility and an unexpected low Curie constant. This phase also presents a first-order structural transition above room temperature accompanied by magnetic and electronic transitions. This work opens up a new research domain in the field of strongly electron-correlated materials. From the electrochemical point of view this system may be at the origin of an entire material family optimized by cationic substitutions.